

## Supporting Information

### **Solvent-Free In Situ Self-Nanoemulsifying Dissolving Microneedles for Rapid and Safe Transdermal Treatment of Acute Pain with Plant-Derived Eugenol**

Peiya Shen, Chengxiang Luo, Jiaqi Liu, Desen Wang, Jianjun Zhang, Mi Tang, Shuai Qian \*, Yuan Gao \*, Yuanfeng Wei \*

**Abstract:** Acute pain treatment is often limited by delayed onset and gastrointestinal side effects of NSAIDs, as well as the addiction potential of opioids. Eugenol (EUG), a natural plant-derived compound with rapid analgesic and anti-inflammatory effects, offers a safer alternative but is restricted by gastrointestinal irritation. Here, we developed a surfactant-free self-emulsifying dissolving microneedle (DMN) system based on an amorphous solid dispersion of EUG. Amphiphilic PVP VA64 mediates interfacial interactions at the oil-water interface, enabling in situ nanoemulsion formation upon contact with interstitial fluid, promoting rapid transdermal drug release and efficient skin permeation. In vivo, the DMN achieved a  $T_{\max}$  of ~25 min, inhibited acetic acid-induced writhing by  $72.5 \pm 4.3\%$ , and reduced formalin-induced pain in the second phase by  $68.9 \pm 5.1\%$ , significantly outperforming oral NSAIDs (writhing inhibition:  $45.3 \pm 3.8\%$ , formalin second phase:  $42.6 \pm 4.0\%$ ). This innovative DMN platform provides a safe, efficient, and clinically translatable strategy for the transdermal management of acute.

## **1. Experimental Procedures**

### **1.1 Materials**

Eugenol (EUG, purity: 98.5%) and indomethacin (IDM, purity: 99%) were purchased from Shanghai Yuanye Bio-Technology Co., Ltd. (Shanghai, China). Polyvinylpyrrolidone (PVP K90, Mw: 1000 kDa) and vinyl pyrrolidone-vinyl acetate copolymer (PVP VA64, Mw: 60 kDa) was gifted from BASF Pharm Co., Ltd. (Ludwigshafen, Germany). Polyvinyl alcohol (PVA MXP, Mw: 32 kDa) was obtained from Merck (Darmstadt, Germany). Fluorescent Red 4B (Solvent red 149) was purchased from Ranbar (Pennsylvania, USA). 0.5% Methylene blue solution (CAT: G1302) was purchased from Solarbio Science and Technology Co., Ltd. (Beijing, China). Formalin sodium chloride solution (10%) was purchased from Beijing Mreda Technology Co., Ltd (Beijing, China). Bayaspirin® was purchased from Bayer Healthcare Co., Ltd (Beijing, China).

### **1.2 Design and preparation of EUG-loaded dissolving microneedle (DMN)**

#### **1.2.1 Tip part of EUG-loaded DMN**

EUG-PVP VA64-PVP K90 ASD made by a co-rotating twin-screw extruder (PPS TSE Elf, Suzhou Pupeishan Technology Co., Ltd, China) with a functional length of 20:1 L/D and a die opening of 3 mm diameter was used to prepare the tip part of DMNs. PVP VA64, with good biosafety and water solubility<sup>1-3</sup>, not only promotes the release of EUG, but also acts as an "amphiphilic polymer" surfactant attached to the EUG-aqueous medium interface, promoting the formation of SEDDS in the skin ISF<sup>4</sup>. PVP K90, which is also biosafe and water-soluble, can be applied for improving the mechanical strength of DMNs due to its good toughness<sup>5,6</sup>. Briefly, 11.0 g PVP VA64, 9.0 g PVP K90, and 5.0 g EUG were mixed for 10 min using a 3D mixer (SBH-1, Xinbao Co. Ltd., China), and the obtained mixture was added into the hopper at the feeding rate of 1 g min<sup>-1</sup> and screw speed of 40 rpm. The hot-melt extrusion (HME) process was conducted using a four-zone barrel. The feeding zone (zone I) was maintained at 40 °C for both the tip and backing formulations, while the processing temperatures in zones II-IV were set at 160 °C for the tip part and 180 °C for the backing part, respectively.

#### **1.2.2 Backing part of EUG-loaded DMN**

PVP VA64-PVA MXP extrudate obtained via a co-rotating twin-screw extruder was used to make the backing part of DMNs, in which the water-soluble PVA MXP has better adhesion after water absorption thus preventing DMNs from coming off the skin<sup>7,8</sup>. Briefly, 10.0 g PVP VA64 was mixed with 10.0 g PVA MXP for 10 min by a 3D mixer and then added into the hopper at the feeding rate of 1 g

min<sup>-1</sup> and screw speed of 40 rpm. The above extrudates were collected on an aluminum plate accompanied with cooling to room temperature, respectively. Further, the cooled extrudates were ground with mortar, and finally passed through a sieve of 60 mesh to obtain the final powders for preparing DMNs.

### **1.2.3 Fabrication process of EUG-loaded DMN**

A polydimethylsiloxane (PDMS) microneedle mold with a four-pronged conical tip, a needle length of 900  $\mu\text{m}$ , a base area of 420  $\mu\text{m}$ ×420  $\mu\text{m}$  for a single microneedle, and a number array of 20×20 was used in this study. DMNs were prepared using the HME technique combined with hot embossing method, which is a simple process without the introduction of organic reagents. The specific process was as follows (Figure S1): (1) about 0.5 g EUG-PVP VA64-PVP K90 ASD powder was filled into the mold, covered with a mold lid and a glass plate, and further pressurized under 1.0 MPa; (2) it was heated in a electro-thermal blast drying oven (DHG-9015A, Shanghai One Instrument Science Instrument Co., Ltd, China) at 160°C for 10 min; (3) the mold was removed from the drying oven, then the fixture was removed and excess melt outside the tip portion of the mold was scraped off; (4) after cooling at room temperature, about 0.5 g of PVP VA64-PVA MXP extrudate powder was filled into the backing portion in the mold. Then, the EUG-loaded DMN was finally demolded after heating at 180°C for 10 min and then cooling at room temperature using the same method described above.

## **1.3 Characterizations of EUG-loaded DMN**

### **1.3.1 HPLC method**

The contents of EUG in freshly prepared EUG-PVP VA64-PVP K90 ASD and EUG-loaded DMN were analyzed by HPLC method (LC-2010A HT, SHIMADZU, Japan) at 280 nm<sup>9</sup>. The mobile phase consisted of 70% methanol and 30% pure water. The separation was conducted on an Ultimate-C18 column (250.0×4.6 mm, 5.0  $\mu\text{m}$ , Waters, USA) with a column temperature of 30°C at a flow rate of 1.0 mL min<sup>-1</sup>.

### **1.3.2 Gas chromatographic analysis**

Gas chromatographic analysis was performed using an Agilent GC-8890 system (Agilent Technologies, USA) equipped with a flame ionization detector (FID) and a SH-WAX capillary column (30 m × 0.25 mm × 0.25  $\mu\text{m}$ ). EUG reference standard was accurately weighed, dissolved in n-hexane, and diluted to 10 mL to obtain a final concentration of 2.3 mg/mL. One EUG-loaded DMN patch was placed into a volumetric flask containing approximately 25 mL of n-hexane, and the total weight was recorded. The mixture was sonicated for 15 min, cooled to room temperature, and replenished with n-hexane to

restore the initial weight. The resulting solution was filtered, and the filtrate was used for GC analysis. Chromatographic conditions were as follows<sup>10</sup>: injection volume, 1  $\mu$ L; split ratio, 20:1; injector and detector temperatures, 230 °C and 280 °C, respectively; carrier gas, high-purity nitrogen at a constant linear velocity of 30 cm/s (initial flow rate 0.94 mL/min); and oven temperature maintained isothermally at 190 °C for 16 min. This method enabled stable and reproducible quantification of EUG in the microneedle matrix.

### **1.3.3 Headspace solid-phase microextraction gas chromatography-mass spectrometry**

For the headspace solid-phase microextraction gas chromatography-mass spectrometry (HS-SPME-GC-MS) analysis<sup>11</sup>, the microneedle tips were carefully scraped, and the sample was accurately weighed to 2.0 g (to four decimal places). The sample was then placed into a 20 mL headspace vial. Automated headspace solid-phase microextraction was performed using a PAL RTC autosampler (CTC Analytics AG, Switzerland). The extraction was carried out using a PA-85  $\mu$ m fiber (Merk) at an extraction temperature of 70 °C for 30 minutes, after a 2-minute equilibrium at 70 °C. The extracted sample was desorbed for 6 minutes at 250 °C before analysis. Gas chromatography-mass spectrometry (GC-MS) analysis<sup>12</sup> was conducted using a Shimadzu QP2010 ultra system (Kyoto, Japan). Chromatographic separation was achieved with an Agilent J&W Scientific DB-5MS capillary column (30 m  $\times$  0.25 mm  $\times$  0.25  $\mu$ m). The injector temperature was set at 250 °C with a split ratio of 50:1, and helium gas was used as the carrier gas at a flow rate of 1 mL/min. The temperature program was as follows: initial temperature of 60 °C held for 1 minute, then increased at a rate of 4 °C/min to 220 °C, where it was held for 30 minutes. The ion source temperature was set to 200 °C, and the interface temperature was set to 250 °C, with a scanning range of m/z 33-500. For identification purposes, 0.2  $\mu$ L of eugenol standard was directly injected and analyzed using the same GC-MS method.

### **1.3.4 True density test**

The true density of EUG-PVP VA64-PVP K90 ASD powder was determined by gas displacement method (Automatic true density analyzer, Ultrapyc 1200e, Quantachrome, USA). Prior to sample testing, the air pressure was adjusted to 21.5 psi and the sample compartment volume was calibrated. The analytical conditions were set to a purge count of 10, a purge fill pressure of 19.5 psi, an analytical count of 10, an analytical fill pressure of 19.5 psi, and an equilibrium condition of 0.001 psi. About 3.5 g of EUG-PVP VA64-PVP K90 ASD powder was placed in the tester with nitrogen as the medium. Ten

parallel determinations were made and the average of the last three was taken as the final determination.

### 1.3.5 Scanning electron microscope (SEM)

The actual geometry of the needle tip in EUG-loaded DMN was measured by SEM (VEGA3, TESCAN, Czech). The accelerating voltage was set to 20 kV. The surface of the needle tip was gold sprayed under vacuum conditions before observation. The SEM images were analyzed using Image J software (version 2) to calculate the actual volume of the tip. Further, the theoretical content of EUG in the needle tip was calculated by combining the value of EUG content in EUG-PVP VA64-PVP K90 ASD measured in 1.3.1 and the true density value of EUG-PVP VA64-PVP K90 ASD measured in 1.3.2, as shown in Equation (1):

$$m = c \times \rho \times \frac{1}{3} \times s \times h \times 400 \quad (1)$$

where  $\rho$  is the true density value of EUG-PVP VA64-PVP K90 ASD,  $S$  is the bottom area of a single microneedle,  $h$  is the height of a single microneedle, 400 is the number of microneedles on the microneedle patch, and  $c$  is the measured content of EUG in EUG-PVP VA64-PVP K90 ASD.

### 1.3.6 Stereomicroscope

The prepared EUG-loaded DMN was placed under a stereomicroscope (AXio200mV.16, Zeiss, Germany) to observe whether the array was intact or not, and whether the tip of the needle was bent or broken.

### 1.3.7 Differential scanning calorimetry (DSC)

Thermal behaviors of the samples, including PVP VA64, PVP K90, and the tip section of EUG-loaded DMN, were investigated by DSC (DSC 250, TA Instruments, USA). Each sample (3.0-5.0 mg) was placed in a sealed aluminum pan and then heated in the range of 20~200°C with a rate of 10°C min<sup>-1</sup> under the nitrogen flow of 50 mL min<sup>-1</sup>. Data were analyzed using TRIOS software (version 5.1.1), including T<sub>g</sub> and melting temperature (T<sub>m</sub>) values.

### 1.3.8 X-ray diffraction (XRD) analysis

XRD analysis was used to gain more insights into the structure information of samples using an X-ray diffractometer (D/max 2500, Rigaku Co., Tokyo, Japan) with Cu-K $\alpha$  radiation of 1.5406 Å. The diffractometer was operated with a fixed tube current (100 mA) and voltage (40 kV). Samples were placed in an aluminum holder, and their PXRD patterns were collected from 5 to 40° 2 $\theta$  with a scanning

speed of 10° min<sup>-1</sup> and a step size of 0.02°.

#### **1.3.9 Fourier transform Raman spectroscopy (FT-Raman)**

FT-Raman spectra of samples were recorded using a Thermo DXR laser confocal Raman spectrometer (Thermo Scientific DXRxi, Thermo Fisher Scientific, USA) with a 785 nm excitation laser. A total of 16 scans were performed in the range of 1400-3406 cm<sup>-1</sup> with a spectral resolution of 4.7 cm<sup>-1</sup>.

#### **1.4 Mechanical characterization**

All in vivo experiments were licensed and ethically approved by China Pharmaceutical University (approval/accreditation number: 2022-08-016) and conducted in accordance with Guidelines for Ethical Review of Laboratory Animal Welfare. Male KM mice, weighing 25±5 g, were acclimatized for at least 1 week and fed ad libitum before experiment. Ethical approval to conduct in vivo experiments was granted by the China Pharmaceutical University Animal Ethics Committee. Animals were operated on and handled according to the guidelines for the care and use of laboratory animals. After KM mice were executed by cervical dislocation, their back skin was shaved and coated with depilatory cream and finally wiped clean with saline. The depilated back skin was clipped and laid flat on a tabletop with the cuticle facing up. The prepared EUG-loaded DMN was pressed onto the skin with the thumb for 30 s and then removed, followed by staining the pinhole array area with 0.5% methylene blue solution for 5 min, and the residual solution was wiped with an alcohol cotton pad. A stereomicroscope (AXio200mV.16, Zeiss, Germany) was used to observe the pinhole staining situation left by DMN on the skin.

#### **1.5 Skin barrier restoration properties**

Skin stratum corneum recovery was often evaluated in terms of pore closure<sup>13</sup>. Male mice were injected intraperitoneally with 0.5 mL of 1.25% tribromoethanol<sup>14</sup>. After the mice were anesthetized, their back skin was shaved and coated with depilatory cream and finally wiped clean with saline water. The EUG-loaded DMN was pressed onto the dorsal skin with the thumb for 30 s and then removed, and the skin recovery was observed at different time points after the removal of DMN.

#### **1.6 Mechanical strength test**

A quarter of the microneedle patch (10 × 10 array) was placed on the stage of an electronic universal testing machine (E45, MTS, USA) due to equipment size limitations. A P/20 cylindrical probe was applied

vertically at a constant speed of 20 mm/min to compress the microneedle tips. The test was stopped when the needle deformation reached 700  $\mu\text{m}$ , and the corresponding force-displacement curve was recorded to assess the mechanical behavior.

### **1.7 In vitro drug release test**

Dissolution tests were conducted in triplicate by a small-volume dissolution apparatus (RC-806ADK dissolution tester, TDTF Technology Co., Ltd, China) at 32°C. The dissolution tests were performed in 20 mL PBS medium with pH 7.4. The foam block was adhered to the backing of a piece of DMN and then dropped into the dissolution cup, relying on buoyancy to ensure that the tip portion of DMN was directed toward the medium, as shown in Figure 3Ab. Samples were pipetted 1 mL at the sampling points (3, 5, 10, 15, 20, 30, 45, 60, 120, and 180 min), immediately followed by isothermal equivalents of fresh media replenished to the dissolution cup. EUG concentration was determined by the HPLC method as described in section 1.3.1 after filtration through a 0.45  $\mu\text{m}$  polyethersulfone membrane filter (Millipore, Bedford, MA). To further elucidate the dissolution behavior of DMNs during drug release, the microneedle morphology was examined at selected time points (10, 30, and 60 min) using a stereomicroscope. This morphological observation provided visual evidence correlating the physical dissolution of the DMN matrix with its drug release profile.

### **1.8 Diffusion behavior of EUG in isolated skin**

About 30 mg of Runbar fluorescent Red 4B powder was dissolved in 2 g EUG, and then the fluorescently labeled EUG was prepared as DMN according to the method in 1.2. Then, after the dehairing treatment, the DMN was pressed onto the isolated dorsal whole skin of mice and fixed with medical tape as a sample group. Approximately 1 mL of EUG-PVP VA64-PVP K90 control solution was applied to the isolated dorsal whole skin of mice as a control group, in which the control solution was prepared by vortexing 50 mg of fluorescently labeled EUG, 110 mg of PVP VA64, and 90 mg of PVP K90 in 10 mL of purified water for 10 min. After 30 min, the DMN was removed as well as the control solution was erased, and the isolated dorsal whole skins of mice were fixed with 4% paraformaldehyde solution for 24 h at room temperature. The samples were embedded in paraffin and cut longitudinally into 3  $\mu\text{m}$ -thick slices, followed by paraffin removal by hydration to avoid its fluorescence from affecting the experimental results. Then, the above sections as well as fluorescently labeled DMN were observed by fluorescence microscope (DM-2500, Leica, Germany). The specific experimental procedure is shown in

Figure 3C.

### 1.9 Dynamic light scattering (DLS)

To monitor the formation and stability of self-emulsifying nanoparticles released from the EUG-loaded DMN, DLS measurements were performed on samples collected during the in vitro drug release study (as described in Section 1.6). Briefly, at predetermined time points (10, 30, 60, and 180 min), 2 mL aliquots of the dissolution medium containing released EUG and self-emulsifying nanoparticles were collected and immediately analyzed by DLS (NanoBrook Omni, Brookhaven, USA) at 25°C in a quartz fluorometer cell at a 90° scattering angle. Each measurement was performed for 1.5 min and repeated three times to obtain the average hydrodynamic diameter and particle size distribution. After sampling, an equal volume of fresh medium was replenished to maintain constant dissolution conditions.

### 1.10 Transmission electron microscopy (TEM)

The morphology of EUG-loaded DMN during dissolution was observed under TEM (HT7700, Hitachi, Japan) with an accelerating voltage of 120 kV. Under the same dissolution test conditions as 1.8, about 2 µL of sample was collected at 1 h and was deposited onto the carbon-coated copper grids. Then, the excess sample was aspirated after 10 min of incubation, followed by secondary staining of the copper grids with a 2% phosphotungstic acid solution for 3 min each time, and dried under an infrared lamp before imaging. The obtained images were evaluated for particle size using Image J software (version 2) and further fitted with Gaussian by Origin 2019b software to obtain the particle size distribution and average particle size values.

### 1.11 Small-angle X-ray scattering

The structure of the emulsion droplets formed during the dissolution of the EUG-loaded DMN was determined by Xeuss SAXS/WAXS system (Xenocs, France) with  $\lambda=0.154$  nm<sup>15,16</sup>. Under the same conditions as described in section 1.7 (In vitro drug release test), approximately 1 mL of the DMN dispersion was collected after 1 h for small-angle X-ray scattering (SAXS) analysis. About 100 µL of the sample was placed onto a glass plate secured with polynicotinamide tape and positioned on the sample holder in the instrument chamber. The SasView software (version 4.1.2) was used to analyze the obtained small-angle X-ray scattering data. The relationship between light scattering vector and light scattering intensity was calculated by the formula:

$$q = (4\pi \cdot \sin\theta) / \lambda. \quad (1)$$



where  $q$  is the scattering vector,  $\vartheta$  is the scattering angle and  $\lambda$  is the X-ray wavelength.

Since the distance between particles was much larger than the size of particles themselves, the interaction between the particles was very weak, and the scattering intensity of particles obeyed Guinier law with the following equation<sup>17,18</sup>:

$$I(q) = I(0) \exp\left[-\frac{q^2 R_g^2}{3}\right] \quad (2)$$

where  $I(0)$  is the scattering intensity at  $0^\circ$ ,  $R_g$  is the radius of gyration,  $q$  is the scattering vector,  $\vartheta$  is the scattering angle and  $\lambda$  is the X-ray wavelength.

### 1.12 Ex vivo transdermal test

The multifunctional transdermal diffusion instrument (SYT-103A1, Yanji Aidi Choke Technology Co., Ltd., China) was used to conduct the in vitro transdermal test of EUG-loaded DMN and EUG-PVP VA64-PVP K90 control solution, where the control solution was prepared by vortexing 25 mg of EUG, 55 mg of PVP VA64, and 45 mg of PVP K90 in 20 mL of purified water for 10 min. Dorsal skin from male KM mice ( $25 \pm 5$  g) was obtained after euthanasia by cervical dislocation, followed by removal of subcutaneous fat and connective tissue. The depilated and prepared skin was then used in the transdermal diffusion cells. The EUG-loaded DMN was pressed with the thumb on the above-treated isolated skins for 30 s. After removing the thumb, the skin was fixed over a receptor compartment containing 4 mL of PBS 7.4. In addition, approximately 1 mL of control solution was added to the donor compartments of four diffusion cells, respectively, where the diffusion cells had fixed with the above-treated isolated skins, as shown in Figure 4A. The temperature of the medium in receptor compartments was set at  $32^\circ\text{C}$  and the rotational speed was set at 600 rpm. About 100  $\mu\text{L}$  of aliquots were withdrawn at predetermined time (3, 5, 10, 15, 20, 30, 45, 60, 120 and 180 min), and then the same volume of fresh buffer was replenished, followed by combining the four samples originating from the same DMN. EUG was extracted from the obtained samples by protein precipitation method, i.e., 400  $\mu\text{L}$  samples were mixed with 800  $\mu\text{L}$  methanol. The mixture was vortexed for 2 min and centrifuged at 12000 rpm for 10 min to obtain the supernatant. EUG concentration was determined by the HPLC method described in section 1.3.1.

### 1.13 In vivo pharmacokinetic study

Male SD rats weighing 180-220 g were acclimatized to the environment for at least 1 week before

the experiment, followed by 24 h of fasting but free access to water. The rats were randomly divided into EUG-loaded DMN group and EUG-PVP VA64-PVP K90 control solution group, with 6 rats in each group. After the backs of rats were depilated, they were anesthetized by intraperitoneal injection of 1.25% tribromoethanol solution ( $10 \text{ mL kg}^{-1}$ )<sup>19</sup>. About 2 mL of EUG-PVP VA64-PVP K90 control solution (preparation method: 25 mg EUG, 55 mg PVP VA64, 45 mg PVP K90 were weighed precisely and vortexed in 10 mL of purified water for 10 min) was applied to the back of rats. Approximately 0.4 mL blood was collected by retro-orbital bleeding at the pre-set time points (5, 10, 25, 25, 45, 60, 120, 180, 210, 240, 270, 300, 420 and 600 min). Plasma samples were placed in centrifuge tubes impregnated with sodium heparin solution and centrifuged at 3000 rpm for 10 min to obtain supernatant plasma, followed by storage at  $-20^{\circ}\text{C}$  for further analysis. EUG was extracted from plasma samples by protein precipitation, i.e., 100  $\mu\text{L}$  of supernatant plasma was mixed with 200  $\mu\text{L}$  of methanol and vortexed for 3 min, followed by centrifugation at 12,000 rpm for 10 min to obtain the supernatant. The details of the method were shown in Figure 4C. The above supernatant samples were analyzed by HPLC method as described in section 1.3.1. To obtain the linear range for the determination of EUG plasma concentration, a standard curve was prepared by adding EUG working standard solutions (20  $\mu\text{L}$  of each concentration of EUG stock solution and 180  $\mu\text{L}$  of methanol) to 100  $\mu\text{L}$  of rat blank plasma, where the concentrations of the mixed solutions were 0.14, 0.28, 0.56, 1.13, 2.25, 4.23, and  $8.45 \text{ mg mL}^{-1}$  (Figure S2, Supporting Information). Subsequent processing was identical to that of plasma samples. Pharmacokinetic parameters were calculated by PK Solver 2.0.

#### **1.14 In vivo acute analgesic effects of EUG-loaded DMN**

##### **1.14.1 Acetic acid writhing test**

The analgesic effect of samples was assessed by the inhibitory effect on acetic acid-induced writhing response in mice<sup>20–23</sup>. KM mice were randomly divided into blank control group, EUG-loaded DMN group, EUG-PVP VA64-PVP K90 control solution group, aspirin suspension positive control group, and indomethacin suspension positive control group, in which 6 mice and half of males and females in each group. The details of examination method were shown in Figure 5A. The blank control group was injected intraperitoneally with acetic acid solution ( $0.6\%$ ,  $10 \text{ mL kg}^{-1}$ ), and the occurrence of abdominal contraction and hind limb extension was recorded as one torsion, and the number of torsions of KM mice was recorded over a 30-minute period. The backs of mice in EUG-PVP VA64-PVP K90 control solution group and EUG-loaded DMN group were depilated. The EUG-loaded DMN was pressed on the

back of mice with the thumb for 30 s, followed by fixing the DMN using medical tape. Approximately 2 mL of EUG-PVP VA64-PVP K90 control solution was pipetted and applied to the backs of mice. The mice in the aspirin suspension ( $1 \text{ mg mL}^{-1}$ ,  $15 \text{ mg kg}^{-1}$ ) and indomethacin suspension ( $1 \text{ mg mL}^{-1}$ ,  $10 \text{ mg kg}^{-1}$ ) positive control groups were gavaged. Thirty minutes after administration, an acetic acid solution was injected intraperitoneally into the four groups of mice, and the number of writhing was recorded within 30 min. Further, the analgesic effect of samples was determined by the analgesic percentage value, which was calculated as follows: (number of writhing times in the blank control group - number of writhing times in the administered group)/number of writhing times in the blank control group $\times 100\%$ .

#### **1.14.2 Formalin murine model of pain**

The analgesic effect of samples was assessed by observing the inhibition of plantar responses in formalin-induced mice. The plantar response of formalin-induced mice was divided into two phases, during which there was a resting period, and the two phases had different durations and pain mechanisms<sup>20,24</sup>. The first phase (0-5 min post-injection) was pain induced by the direct activation of both low threshold mechanoreceptive and nociceptive primary afferent fibers, and the second phase (15-35 min post-injection) was pain induced by the inflammatory phenomena within the dorsal horn neurons<sup>25,26</sup>. Drugs with anti-inflammatory mechanisms for analgesia will only be effective in the second phase. Therefore, the formalin test can provide a reference for evaluating the scope of EUG-loaded DMN analgesic adaptation. The details of experimental method were shown in Figure 5A. The sample groups with the corresponding administration methods were the same as those of the acetic acid writhing test. Thirty minutes after administration, mice in the four administration groups were injected with formalin solution (2.5%, 20  $\mu\text{L}$ ) plantarly. The total time the mice licked or bit the plantar (injected plantar) was recorded at two stages (0~5 min and 15~30 min after injection). Then, the analgesic effect of samples was judged by the analgesic percentage, which was calculated as (plantar reaction time of the blank control group - plantar reaction time of the administered group)/plantar reaction time of the blank control group $\times 100\%$ .

#### **1.15 Safety evaluation of EUG-loaded DMN**

Whether EUG-loaded DMN would cause irritation to skin tissues was assessed by Hematoxylin-eosin staining (H&E staining)<sup>27,28</sup>. Male KM mice were injected intraperitoneally with 0.5 mL of 1.25% tribromoethanol, and their back hair was removed after the mice were anesthetized. The DMN was pressed with the thumb on the back of the mice for 30 seconds, then the DMN was secured with medical tape and removed from the back of three mice after 30 minutes, 1 h, and 3 h, respectively. The dorsal skin was clipped and placed in an embedding box and fixed with 4% paraformaldehyde solution at room temperature for 24 h. The fixed samples were embedded in paraffin wax, cut into 3  $\mu\text{m}$ -thick sections, and then stained using the H&E method. Finally, the inflammatory reaction of the skin tissue was observed by microscope (Eclipse Ci-POL, Nikon, Japan).

### 1.16 Statistical analysis

Results were expressed as mean  $\pm$  standard deviation. Significance of difference was analyzed using one-way ANOVA, followed by Tukey's multiple comparisons post test via IBM SPSS® software (Version 26, SPSS Inc., USA). Statistical significance was determined at  $*P < 0.05$ ,  $**P < 0.01$ , and  $***P < 0.001$ . "#" symbols indicate significant differences between each treatment group and the control group ( $#P < 0.05$ ,  $##P < 0.01$ ,  $###P < 0.001$ ).

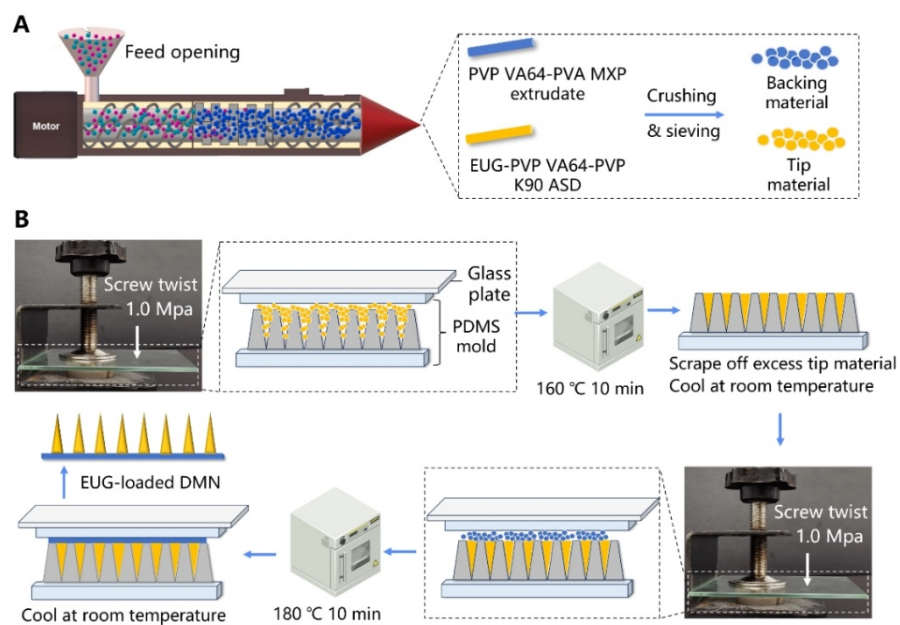
### 1.17 Molecular dynamics (MD) simulation and radial distribution function (RDF) analysis

MD simulations were conducted to elucidate the intermolecular interactions among the components within the microneedle tip. RDF analysis derived from MD simulation provides structural insights by calculating the local spatial distribution and determining the probability density function  $g(r)$ , which describes the likelihood of finding other atoms at a certain distance from a reference atom<sup>29</sup>. All simulations were performed using the Amorphous Cell and Forcite modules of Materials Studio 8.0 with the COMPASS II force field. The van der Waals and electrostatic interactions were computed using the atom-based and Ewald summation methods, respectively. A time step of 1 fs and a total simulation time of 400 ps were employed under NPT and/or NVT ensembles. The detailed simulation procedure was as follows: (1) The molecular structures of EUG, PVP VA64, and PVP K90 were geometrically optimized prior to MD simulation. (2) Amorphous cells containing the three components were constructed and subjected to energy minimization. (3) Dynamic simulations were subsequently carried out under NPT and NVT ensembles at 160 °C using the Andersen thermostat, to mimic the microneedle preparation conditions. (4) Quenching simulations were then performed under the NVT ensemble at 25 °C. (5) After equilibration, RDF analyses were conducted to calculate the  $g(r)$  values between electron donor and acceptor groups among the components using the Analysis function in the Forcite module.

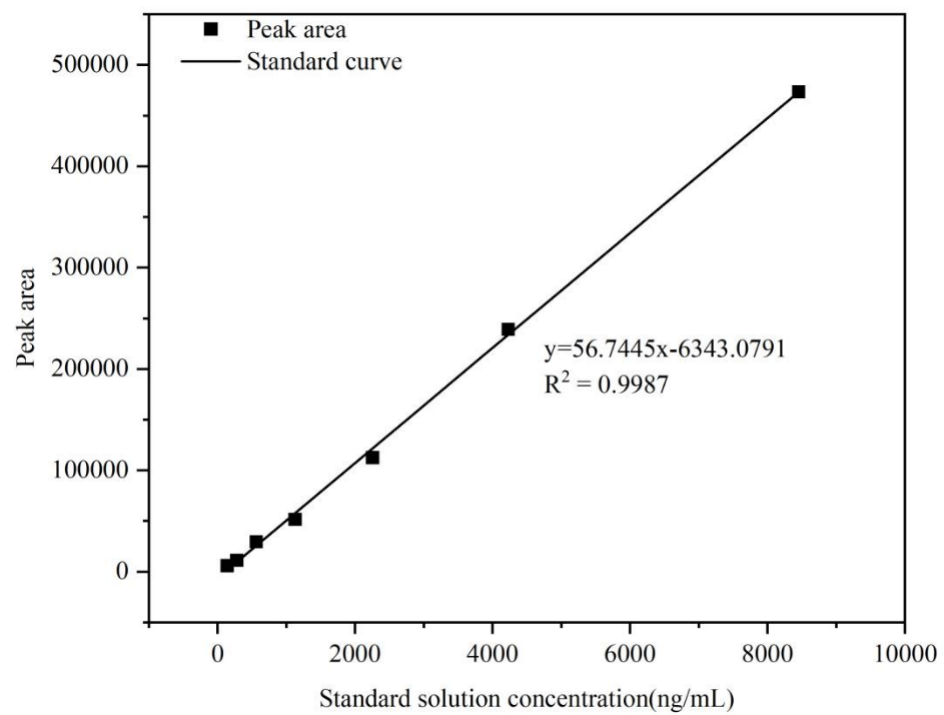
## 2. Information about electronic supplementary material

Figure S1. Schematic diagram of the preparation process of EUG-loaded DMN. Figure S2. EUG concentration versus peak area of drug standard curve for drug plasma concentration calculation. Figure S3. Radial distribution function (RDF) plots illustrating hydrogen-bonding interactions between EUG and PVP VA64. Figure S4. Gas chromatogram and HS-SPME-GC-MS analysis of pure EUG reference standard and EUG extracted from the EUG-loaded DMN tips. Figure S5. FT-Raman spectra of EUG, PVP K90, PVP VA64, and the tip material of EUG-loaded DMN. Figure S6. X-ray diffraction (XRD) profiles of the tip material of EUG-loaded DMN. Figure S7. Small-angle X-ray scattering profiles of emulsion

droplets formed after dissolution of EUG-loaded DMNs for 1 h in 20 mL PBS medium (pH 7.4). Figure S8. Force-displacement profile of EUG-loaded DMN during the compression test. Figure S9. Characterization and molecular interaction analysis of EUG-loaded DMN under simulated interstitial fluid (ISF) conditions. Table S1. PDI values of EUG-loaded DMN at different time points at 32 °C PBS 7.4 medium. Table S2. The long and short diameters of the emulsion droplets formed by EUG-loaded DMN in TEM image. Table S3. Pharmacokinetic parameters of EUG-loaded DMN and EUG-PVP VA64-PVP K90 control solution. Table S4. Number of writhes and analgesic rate in the acetic acid-induced writhing test. Table S5. Paw-licking time and analgesic rate in the formalin test.



**Figure S1.** Schematic diagram of the preparation process of EUG-loaded DMN. (A) Preparation of needle tip and backing material by HME technique; (B) Preparation of EUG-loaded DMN by hot embossing method.



**Figure S2.**EUG concentration versus peak area of drug standard curve for drug plasma concentration calculation.

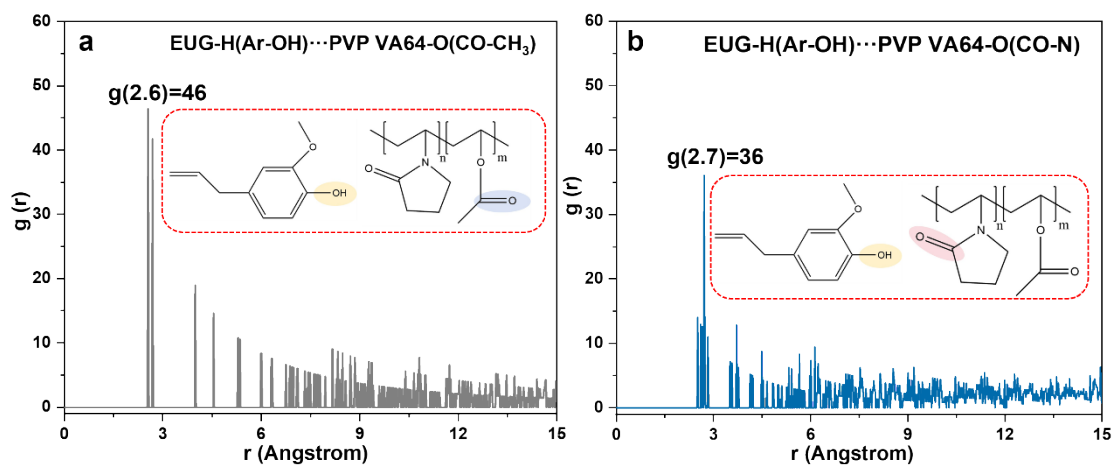


**Figure S3.** Radial distribution function (RDF) plots illustrating hydrogen-bonding interactions between the phenolic hydroxyl group of eugenol (EUG) and (a) the carbonyl group of the pyrrolidone moiety in PVP VA64, and (b) the carbonyl group of the ester linkage in PVP VA64.



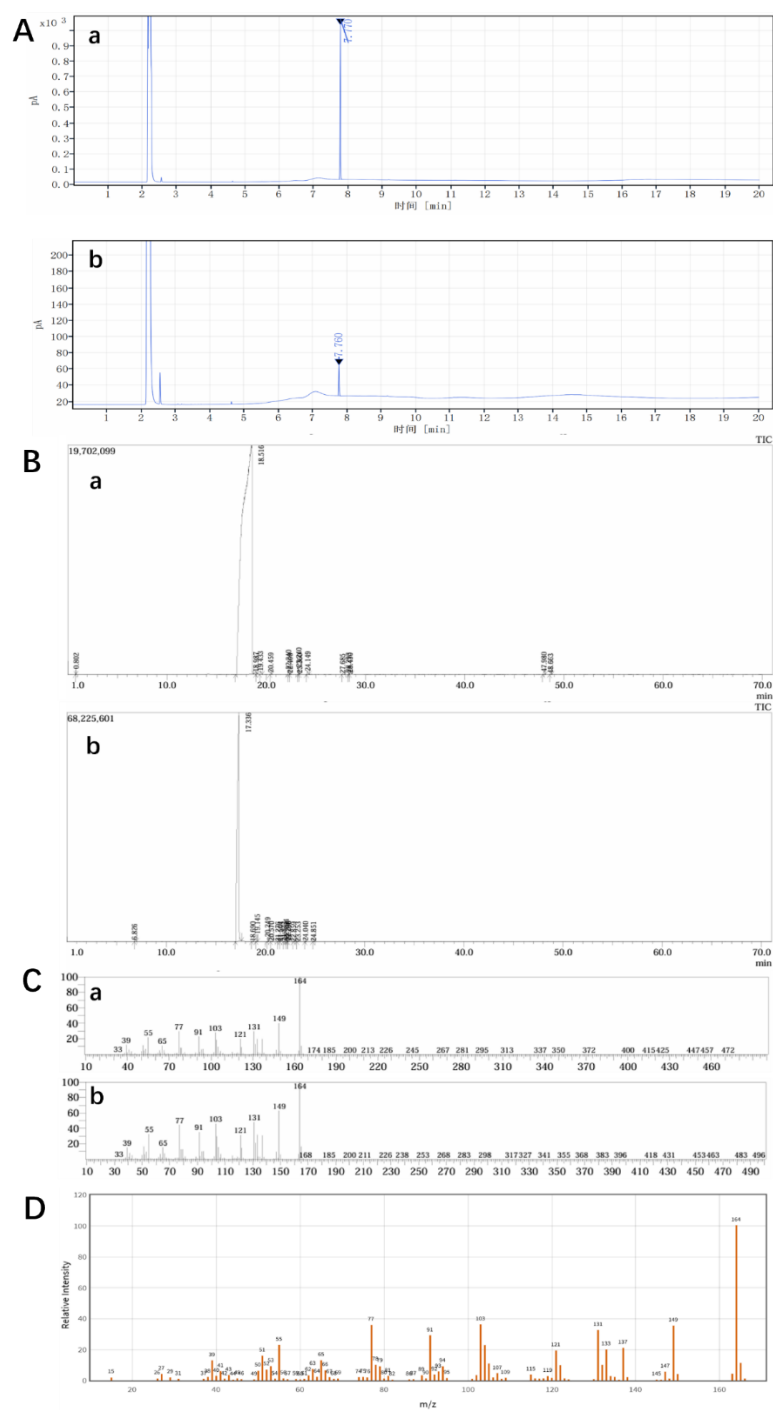


**Figure S4.** (a) Gas chromatogram of pure eugenol (EUG) reference standard. (b) Gas chromatogram of EUG extracted from the EUG-loaded dissolving microneedle (DMN) tips. B. The chromatograms show consistency in the retention times of the main peaks between the DMN sample (a) and the standard EUG (b). C. Corresponding mass spectra, (a) mass spectrum of EUG from the DMN sample, (b) mass spectrum of the standard EUG. D. Standard mass spectrum of EUG from the NIST database.

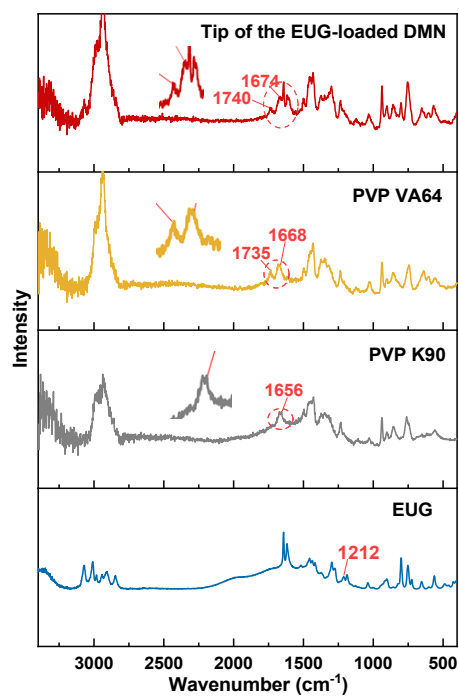


**Figure S5.** FT-Raman spectra of EUG, PVP K90, PVP VA64, and the tip material of EUG-loaded DMN.

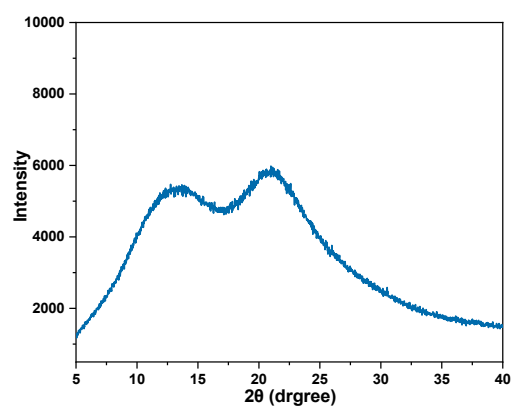


**Figure S6.** X-ray diffraction (XRD) profiles of the tip material of EUG-loaded DMN.

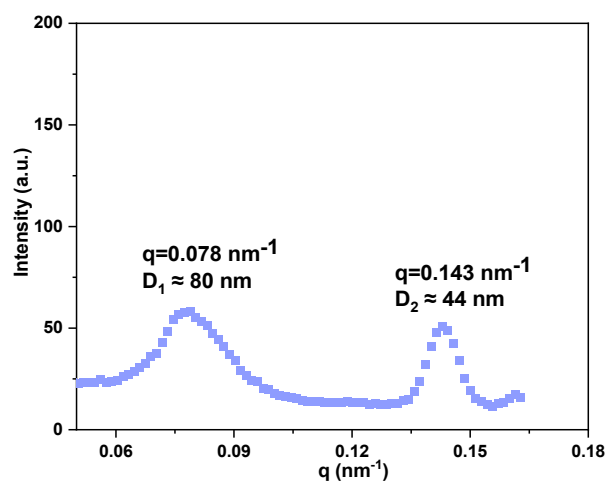


**Figure S7.** Small-angle X-ray scattering profiles of emulsion droplets formed after dissolution of EUG-loaded DMNs for 1 h in 20 mL PBS medium (pH 7.4).

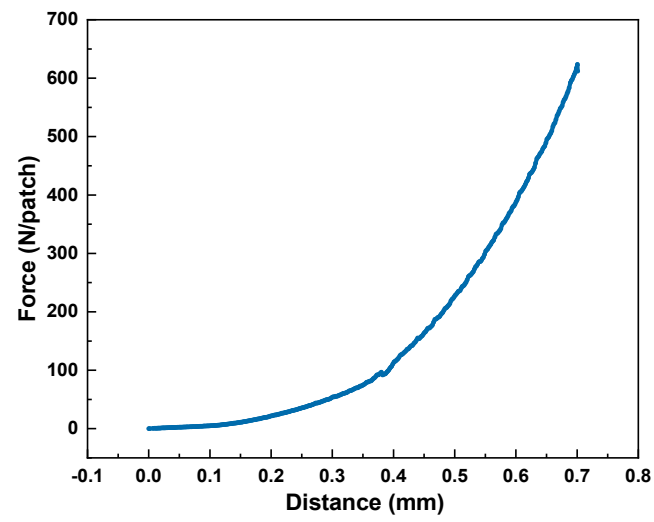


**Figure S8.** Force-displacement profile of EUG-loaded DMN during the compression test.

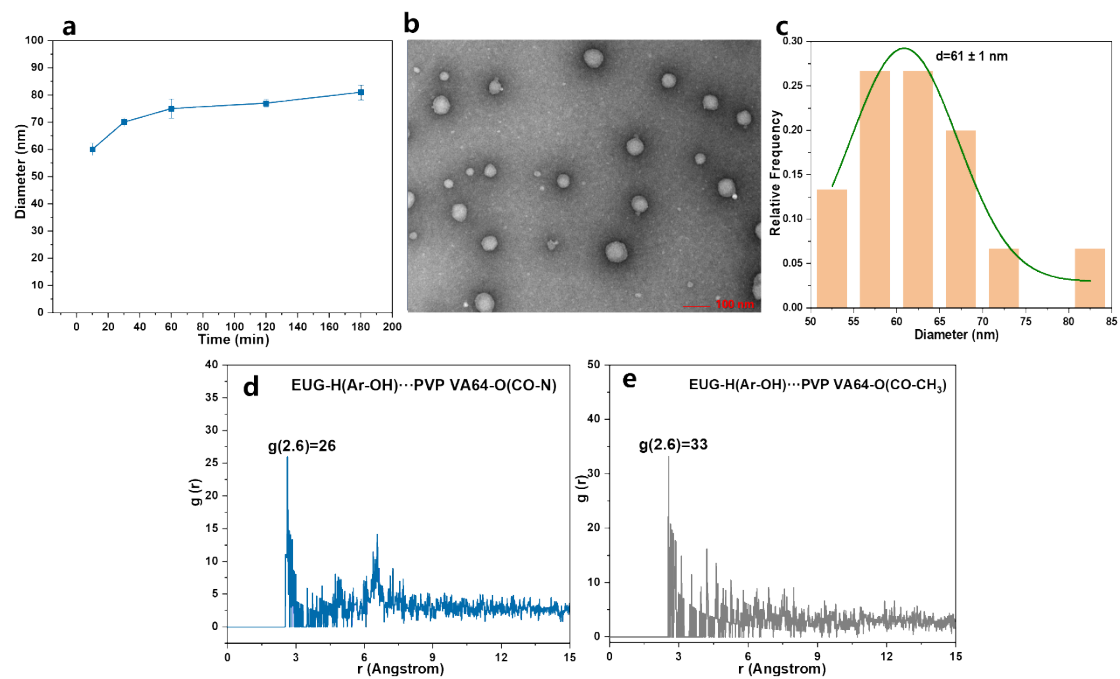


**Figure S9.** Characterization and molecular interaction analysis of EUG-loaded DMN under simulated interstitial fluid (ISF) conditions. (a) DLS profile of EUG-loaded droplets in artificial ISF. (b) TEM image of droplets in protein-free ISF. (c) Gaussian distribution analysis of droplet size corresponding to (b). (d, e) Radial distribution function (RDF) analysis of hydrogen-bond interactions between EUG and PVP VA64.

**Table S1.** PDI values of EUG-loaded DMN at different time points at 32°C PBS 7.4 medium (n=3, mean±SD).

Time	EUG-loaded DMN
10 min	0.299±0.009
30 min	0.292±0.060
1 h	0.212±0.031
3 h	0.293±0.007

**Table S2.** The long and short diameters of the emulsion droplets formed by EUG-loaded DMN in TEM image.

EUG-loaded DMN 1 h 20K			
Number	Width (nm)	Height (nm)	Average (nm)
1	119.5	115.6	117.6
2	68.1	67.0	67.6
3	79.4	84.8	82.1
4	77.7	80.8	79.3
5	76.6	68.1	72.4
6	71.6	74.5	73.1
7	75.5	74.4	75.0
8	75.5	74.5	75.0
9	79.8	81.2	80.5
10	82.1	84	83.1
11	88.3	85.1	86.7
12	71.9	77.7	74.8
13	85.1	80.8	83.0
14	70.2	69.1	69.7
15	79.4	83.3	81.4
16	84.4	82.9	83.7
17	61.3	59.6	60.5
18	65.9	68.4	67.2
19	68.1	66.7	67.4
20	78.0	69.5	73.8
21	59.9	65.9	62.9
22	73.7	70.9	72.3
23	52.8	56.7	54.8
24	57.8	62.8	60.3
25	48.6	44.7	46.7
26	41.1	39.7	40.4
27	39.4	37.9	38.7
28	34.0	31.2	32.6



**Table S3.** Pharmacokinetic parameters of EUG-loaded DMN and EUG-PVP VA64-PVP K90 control solution<sup>[a]</sup>

	EUG-PVP VA64-PVP K90 Control solution	EUG-loaded DMN
$C_{\max}$ (ng mL <sup>-1</sup> )	1387.80±242.04	2145.68±218.27*
$T_{\max}$ (min)	45.00	25.00
$t_{1/2}$ (min)	142.40±5.77	142.44±7.22
$AUC_{0-300 \text{ min}}$ (ng mL <sup>-1</sup> min)	22.04×10 <sup>4</sup> ± 30.93×10 <sup>3</sup>	34.42×10 <sup>4</sup> ± 13.14×10 <sup>3</sup> **
$AUC_{0-\infty}$ (ng mL <sup>-1</sup> h)	24.12×10 <sup>4</sup> ± 30.31×10 <sup>3</sup>	36.96×10 <sup>4</sup> ± 97.02×10 <sup>2</sup> **

[a] The data were expressed as mean ± S.D. \* :  $p < 0.05$ , vs EUG-PVP VA64-PVP K90 control solution; \*\*  $p < 0.01$ , vs EUG-PVP VA64-PVP K90 control solution.

**Table S4.** Number of writhes and analgesic rate in the acetic acid-induced writhing test (n = 6, data are presented as mean  $\pm$  SD).

Group	Number of twists	Percentage of analgesia
Control group	51 $\pm$ 5	/
EUG-loaded DMN	9 $\pm$ 8	82%
Control solution	33 $\pm$ 7	35%
Indomethacin suspension	39 $\pm$ 1	24%
Aspirin suspension	27 $\pm$ 1	47%

**Table S5.** Paw-licking time and analgesic rate in the formalin test (n = 6, data are presented as mean  $\pm$  SD).

Group ( Phase I )	Foot-licking/biting time (s)	Percentage of analgesia
Control group	128.3 $\pm$ 10.3	/
EUG-loaded DMN	123.3 $\pm$ 25.4	4%
Control solution	120.0 $\pm$ 8.2	6%
Indomethacin suspension	121.3 $\pm$ 15.3	5%
Aspirin suspension	111.3 $\pm$ 17.2	13%

Group ( Phase II )	Foot-licking/biting time (s)	Percentage of analgesia
Control group	220.7 $\pm$ 40.2	/
EUG-loaded DMN	67.0 $\pm$ 7	70%
Control solution	132.7 $\pm$ 27.2	40%
Indomethacin suspension	157.3 $\pm$ 42.1	29%
Aspirin suspension	117.0 $\pm$ 10.8	47%

## SI References

- 1 M. Fanous, S. Gold, S. Muller, S. Hirsch, J. Ogorka and G. Imanidis, *Int. J. Pharm.*, 2020, **578**, 119124.
- 2 Y. Guo, H. Patel, A. Saraswat, K. V. Mateti, K. Patel and E. Squillante, *J. Drug Deliv. Sci. Technol.*, 2023, **88**, 104852.
- 3 V. Onesto, C. Di Natale, M. Profeta, P. A. Netti and R. Vecchione, *Prog. Biomater.*, 2020, **9**, 203–217.
- 4 P. Shen, E. Hu, C. Zhang, Y. Gao, S. Qian, W. Heng, J. Zhang and Y. Wei, *Adv. Healthc. Mater.*, 2024, **13**, 2302488.
- 5 S. Bhatnagar, P. R. Gadeela, P. Thathireddy and V. V. K. Venuganti, *J. Chem. Sci.*, 2019, **131**, 90.
- 6 M. Kurakula and G. S. N. K. Rao, *J. Drug Deliv. Sci. Technol.*, 2020, **60**, 102046.
- 7 N. Jain, V. K. Singh and S. Chauhan, *J. Mech. Behav. Mater.*, 2017, **26**, 213–222.
- 8 S. Sau, S. Pandit and S. Kundu, *Surf. Interfaces*, 2021, **25**, 101198.
- 9 S.-M. Yun, M.-H. Lee, K.-J. Lee, H.-O. Ku, S.-W. Son and Y.-S. Joo, *J. AOAC Int.*, 2010, **93**, 1806–1810.
- 10 E. Ertas, A. Aksoy, D. Guvenc, Y. K. Das and A. C. Yucel, *Asian J. Chem.*, 2007, **19**, 3105–3112.
- 11 C. Franc, L. Riquier, X. Hastoy, C. Monsant, P. Noiville, E. Pelonier-Magimel, S. Marchand, S. Tempère, M.-C. Ségur and G. De Revel, *Food Chem.*, 2023, **426**, 136405.
- 12 M. Liang, Z. Yang, K. Xu, X. Chen, J. Yang, W. Liu, S. Zhao, Y. Xu and J. Zhang, *Ital. J. Food Sci.*, 2023, **35**, 69–78.
- 13 T. Y. Han, K. Y. Park, J. Y. Ahn, S. W. Kim, H. J. Jung and B. J. Kim, *Dermatol. Surg.*, 2012, **38**, 1816–1822.
- 14 M. R. Lee, H. R. Suh, M. W. Kim, J. Y. Cho, H. K. Song, Y. S. Jung, D. Y. Hwang and K. S. Kim, *Lab. Anim. Res.*, 2018, **34**, 270.
- 15 T. Li, A. J. Senesi and B. Lee, *Chem. Rev.*, 2016, **116**, 11128–11180.
- 16 Y. Chai, A. Lukito, Y. Jiang, P. D. Ashby and T. P. Russell, *Nano Lett.*, 2017, **17**, 6453–6457.
- 17 Z. Li, N. J. Van Zee, F. S. Bates and T. P. Lodge, *ACS Nano*, 2019, **13**, 1232–1243.
- 18 C. Sofroniou, M. Baglioni, M. Mamusa, C. Resta, J. Douth, J. Smets and P. Baglioni, *ACS Appl. Mater. Interfaces*, 2022, **14**, 14791–14804.
- 19 Y. Cai, P. Lin, Y. Li, L. Liu, S. Cao, B. Zhao, Y. Wang, W. Song, Q. Wang, X. Gan, K. Xu, Q. Wu, Y. Wang, L. Yu and Q. Yuan, *Chem. Eng. J.*, 2024, **502**, 157837.
- 20 M. López-Cano, V. Fernández-Dueñas, A. Llebaria and F. Ciruela, *Bio-Protoc.*, 2017, **7**, 2628.
- 21 C. Camerlingo, Exploring the analgesic potential of isorhamnetin,  
<https://www.europeanreview.org/article/36672>, (accessed October 31, 2025).
- 22 W. Zhao, R. Konno, X.-J. Zhou, M. Yin and Y.-X. Wang, *Cell. Mol. Neurobiol.*, 2008, **28**, 581–591.
- 23 M. L. C. Alvarez, K. M. C. Lim and M. N. Tonog, *J. Pharm. Res. Int.*, 2020, **32**, 58–61.
- 24 *Pain*, 1987, **30**, 103–114.
- 25 S.-H. Park, Y.-B. Sim, J.-K. Lee, S.-M. Kim, Y.-J. Kang, J.-S. Jung and H.-W. Suh, *Arch. Pharm. Res.*, 2011, **34**, 501–507.
- 26 R.-R. Ji, H. Baba, G. J. Brenner and C. J. Woolf, *Nat. Neurosci.*, 1999, **2**, 1114–1119.
- 27 L. Liang, W. M. Fei, Z. Q. Zhao, Y. Y. Hao, C. Zhang, Y. Cui and X. D. Guo, *Eur. J. Pharm. Biopharm.*, 2021, **164**, 20–27.
- 28 H. Chang, S. W. T. Chew, M. Zheng, D. C. S. Lio, C. Wiraja, Y. Mei, X. Ning, M. Cui, A. Than, P. Shi, D. Wang, K. Pu, P. Chen, H. Liu and C. Xu, *Nat. Biomed. Eng.*, 2021, **5**, 1008–1018.
- 29 Z. Shariatnia, in *Modeling and Control of Drug Delivery Systems*, ed. A. T. Azar, Academic Press, 2021, pp. 153–182.